Applied Surface Science Advances 34 (2026) 101033

Contents lists available at ScienceDirect

Applied Surface Science Advances

journal homepage: www.sciencedirect.com/journal/applied-surface-science-advances

Full Length Article

XPS depth profiling of silicon-dioxide/silicon system by means of monatomic and cluster argon ion sputtering

A.S. Racz [a,*], D. Olasz [a,b], M. Menyhard [a,*], O. Krafcsik [a,c]

[a] HUN-REN Centre for Energy Research, Konkoly Thege M. út 29-33, 1121, Budapest, Hungary
[b] Department of Materials Physics, Eötvös Loránd University, Pázmány Péter sétány 1/A, Budapest, 1117, Hungary
[c] Department of Atomic Physics, Institute of Physics, Budapest University of Technology and Economics, Műegyetem rakpart 3., H-1111, Budapest, Hungary

ARTICLE INFO

Keywords:
Silicon-dioxide
XPS
Cluster sputtering
Monatomic sputtering
Atomic mixing

ABSTRACT

Gas cluster ion beams (GCIB) are a relatively new technique for depth profiling organic and sensitive materials. There are only few studies on XPS cluster depth profiling of inorganic materials particularly oxides. In this work a systematic study is presented on a technologically very important system SiO_2/Si which is also regularly applied as a reference in depth profiling studies. In this work clusters of various energies (8 and 6 keV) and of Ar sizes (1000, 500, 150) are used for depth profiling and compared to that of using monatomic (0.5 keV) argon ion sputtering. It is shown that non-stoichiometric silicon oxide is formed at the interfaces, which is the most dominant in the case of cluster of 8 keV 150 while the lowest in the case of cluster of 6 keV 1000. Interestingly in the case of monatomic sputtering the presence of non-stoichiometric oxide remains low compared to other cluster configurations. AFM measurements have shown roughness increase for all cluster depth profiling configurations while only slight roughening was found in the case of monatomic sputtering. Monatomic sputtering still represents a safe alternative for depth profiling inorganics with reasonable sputtering rate.

1. Introduction

Silicon dioxide (SiO_2) thin films on silicon substrates are one of the most important material systems in surface and interface science [1]. Its main application is in semiconductor industry e.g.: is widely used as surface passivation coating in silicon solar cells [2], as dielectric layers [3] and diffusion barriers [4]. With continuous miniaturization of device architectures, oxide thicknesses are mostly in nanometer range, the reliable characterization of thin SiO_2/Si structures are essential for both fundamental studies and technological applications. Moreover, it is frequently used as a substrate for various systems (polymers, semiconductors, metals) and increasingly used as a reference material for sputter rate [5].

X-ray photoelectron spectroscopy (XPS) is a key technique for investigating the chemical composition of nano-layers due to its elemental specificity and chemical-state sensitivity. The technique can be combined with different ion sputtering techniques for investigating deeper regions. During a long time, monatomic ion bombardment was dominantly applied for these tasks. But from the 1980 years works appeared where the single ion has been replaced by clusters (made of solid, liquid or gas atoms) for various aims: smoothing, cleaning, shallow ion implantation etc. [6–8]. From the years of 2000s activity started for the usage of various clusters for XPS depth profiling as well [9,10]. Though both techniques, monatomic and cluster bombardment, are low energy ion bombardments and both cause alterations on the surface and in the surface close regions, still the two mechanisms are strongly different. In the case of monatomic ion bombardment, the energies of the interacting particles generally are higher than 100 eV. Their interaction with the surface can be described by mainly binary interactions and non-interacting thermal spikes. Because of fast relaxation individual events generally do not interact. In the case of cluster bombardment, the energy of the individual particles is much lower than that in case of monatomic bombardment. The energy of the single projectiles is in the range of 3–20 eV, and accordingly the alterations of the surface and surface close region introduced by the individual particle are much weaker than that in the case of monatomic bombardment. On the other hand, in the case of cluster bombardment several interactions occur in the narrow time interval, which allows the interactions among the individual events. It should be also considered that the several keV energy of the cluster absorbs in the surface region, which might cause temperature rise. Thus, it is not easy to tell which of the two methods is to be applied in a certain case. The consensus is that for analysis and /

* Corresponding authors.
E-mail addresses: racz.adel@ek.hun-ren.hu (A.S. Racz), menyhard.miklos@ek.hun-ren.hu (M. Menyhard).

https://doi.org/10.1016/j.apsadv.2026.101033
Received 21 April 2026; Received in revised form 15 June 2026; Accepted 17 July 2026
Available online 22 July 2026

removal of thin organic layers is the field for cluster bombardment, while in the case of inorganic samples such simple statement cannot be made. E. g. considering the important characteristics of the depth profiling procedure like preferential sputtering and depth resolution sometimes behave differently. Until recently, limited work had been published on the use of Ar_n^+gas cluster ion beam (GCIB) sources for XPS depth profiling of inorganic compounds, in particular metal oxides, despite their importance as functional thin films.

To deal with this confused situation Simpson et al. [11] in their seminal paper studied the possibility to apply clusters for XPS depth profiling. They studied the Ar^+ cluster bombardment in the case of Ta_2O_5 layer grown on Ta foil, which is in fact a standard (European standard BCR-261T) for calibrating sputtering rate. It is well known that monatomic sputtering (they used 3 keV and 0.5 keV Ar^+) causes considerable reduction of the oxide because of the preferential sputtering of oxygen and this change reaches a steady state during the sputter removal process. In case of Ar^+ cluster bombardment (6 keV Ar_{1000}^+) they also observed preferential sputtering of oxygen but different from that of monatomic ion sputtering; the composition of the Ta_2O_5 layer continuously varied. In this respect the chemical effect of the cluster bombardment is less than that of monatomic bombardment as expected. On the other hand, the depth resolution was found to be better for monatomic bombardment. Similar results were published by Burrell et al. [12]. They studied the XPS depth profiling of zirconium oxide using cluster and monatomic etching, and found that the chemical damage and depth resolution are better and worst for cluster bombardment compared with monatomic bombardment, respectively. To get the best possible results they used the GCIB sputtering to remove the "bulk" part of the layer and conversing the chemical state, while close to the interface they change for monatomic bombardment to keep to good depth resolution. Barlow et al. [13] studied the chemical damage of the cadmium telluride (CdTe), gallium arsenide (GaAs), gallium phosphide (GaP), indium arsenide (InAs), zinc selenide (ZnSe), hafnium oxide (HfO) due to GCIB treatment. All except one, InAs, of the mentioned compounds were rather resistant to GCIB. InAs on the other hand, it showed serious damage. Moreover, it turned out that in the case of HfO there was no O preferential sputtering. Steinberger et al. have examined FeO and $Zn_5(CO_3)_2(OH)_6$(hydrozincite) using a range of different Ar_n^+CGIB conditions [14]. Preferential sputtering of O was observed both for hydrozincite using Ar_{2000}^+ at incident energies of 4 keV (E/n = 2) and FeO using Ar_{2000}^+ at 6 keV (E/n = 3). Aureau et al. have shown that 4 keV Ar_{3000}^+ does not induce change the chemical state in titanium in single crystal $SrTiO_3$, the strontium has shown a minor chemical change in longer etching time [15]. Thus, one cannot give simple rule concerning the chemical damage of cluster bombardment. It is also important to mention that none of the studies dealt with the morphology development due to cluster sputtering.

Even though the SiO_2/Si system is one of the most intensively studied layer systems, its systematic investigation by XPS depth profiling is very limited. Perhaps only Kyoung et al. investigated the variation of valence band structure of 5 nm SiO_2 thin films during various depth profiling: Ar^+ 0.5 keV/45° and 15 keV Ar_{2500}^+ clusters (0° and 55° with respect the surface normal) [16]. According to the expectation they found that the chemical damage (preferential sputtering) in case of monatomic Ar^+ is the largest. The depth resolution had not been studied and the assessment of different bonding states at the interfaces is missing. The history of monatomic ion bombardment of SiO_2/Si system goes back to decades. On the other hand, Baer et al. [5] used the SiO_2 (thermal oxide) /Si (substrate) system as a standard for determining the relative sputter rate of several commonly used oxides in case of XPS and/or AES depth profiling applying monatomic ion bombardment. The choice of the SiO_2 (thermal oxide) /Si (substrate) system for this purpose is justified by several factors. The most important one is that the semiconductor industry can supply excellent, well-defined samples which are not too sensitive for the monatomic ion bombardment [17] thus, the change of chemistry which might affect the evaluation process see Ref [11] can be ignored.

Herein, XPS depth profiling of a nominally 15 nm SiO_2/Si system made by thermal process is performed using cluster ion sputtering at different energies and cluster sizes and compared with monatomic ion sputtering. This oxide thickness is sufficiently thin to investigate interfacial effects while it is thick enough to monitor the sputtering-induced chemical changes. The influence of sputtering conditions on oxide reduction and interface sharpness is systematically evaluated. Surface morphology development is studied by AFM. As SiO_2 is widespread both as functional material and a reference system in surface analysis, the results might be relevant in the characterization of thin oxide and multilayer systems, as well.

2. Experimental section

2.1. SiO_2/Si production and ellipsometry

The nominally 15 nm thick SiO_2 layer grown on a n-type 100 silicon substrate was produced in an oxidation furnace at 900 °C with an 8 l/min oxygen stream. The thickness of the thermally grown SiO_2 layer was determined by spectroscopic ellipsometry using a Woollam M-2000 ellipsometer. Data were analyzed with the CompleteEase software (v5.15) in the 191–1689 nm wavelength range. A SiO_2 layer (from the built-in library) was used in the optical model on a Si substrate. The thickness of the SiO_2 layer was found to be 14.7 nm.

2.2. Transmission electron microscopy

For investigating the SiO_2/Si interface cross-sectional transmission electron microscopy (XTEM) measurements were performed in a FEI-Themis Cs-corrected transmission electron microscope operated at 200 kV. The sample for XTEM measurement was produced by FIB ion milling in a Thermo Scientific Scios 2 scanning electron microscope. The XTEM image of the sample is depicted in Fig. 1., it reveals a sharp and smooth interface without the presence of any additional interfacial layer.

2.3. XPS depth profiling

The XPS analysis was performed in an Escalab Xi^+ instrument

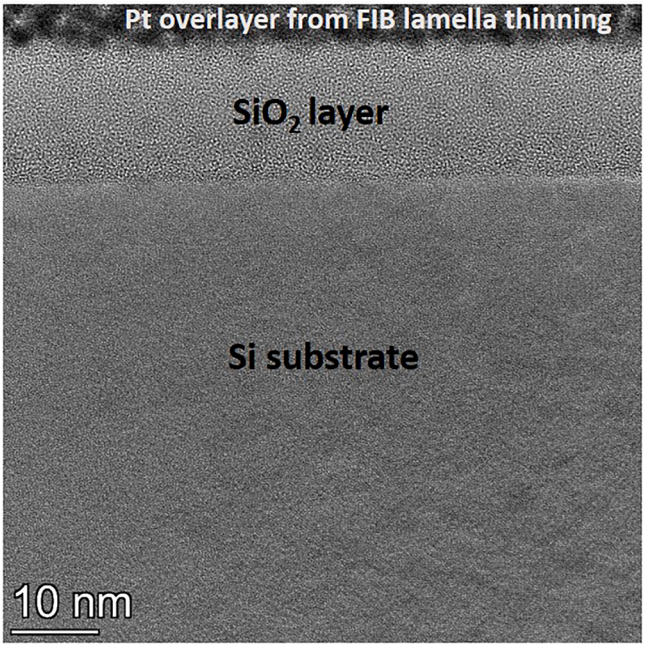

Fig. 1. The XTEM image of SiO_2/Si sub sample.

(Thermo Fisher Scientific). The spectra were recorded applying Al K α X-ray source (1486.6 eV). The size of the X-ray spot was 650 μm, which is much smaller (see later) than that the sputter crater and thus crater effects can be ignored. To reduce charging, the samples were mounted using double-sided carbon tape onto a stainless-steel holder and the carbon tape was additionally extended over the sample surface to ensure electrical contact. In all XPS measurements exactly the same instrumental parameters have been applied. Silicon (2p), carbon (1 s) and oxygen (1 s) high-resolution spectra were measured within the spectral range of interest (ca. 20 eV around the core level emission peaks) at 20 eV pass energies with 0.1 eV steps and 50 ms dwell time per data point. All spectra were collected at normal emission angle. To analyze the change of chemical states during depth profiling, the decomposition of the Si 2p spectrum was applied, since the individual oxidation states (Si^0–Si^{4+}) appear with well-defined chemical shifts. In contrast, the chemical shifts of the O 1 s peak are significantly smaller, and the contributions of the different Si–O bonding environments largely overlap, making it only partially suitable for the reliable identification of Si suboxide components [18,19]. Though we know that sample composition changes within the information depth still as an approximation CasaXPS software [20] (which should apply to homogeneous system) was applied. For decomposing the Si 2p peaks GL(30) peak shapes (Gaussian–Lorentzian product function with a mixing parameter of 30) and Shirley-background subtraction was applied. The elemental Si (Si^0) peak was fitted with a doublet. For the Si^+, Si^{2+}, Si^{3+} and Si^{4+} oxidation states, however, since these peaks are much broader and the components overlap strongly, and the magnitude of the spin–orbit splitting is comparable to the chemical shifts, the resolution of all oxidation states with separate doublets cannot be considered unambiguous. Therefore, each oxidation state was considered with a single peak. To ensure consistent peak fitting, 8 keV Ar^+_{500} depth profile was initially peak fitted to establish the peak fitting parameters with which all subsequent depth profiles were fitted. Fig. 2 shows representative Si 2p spectra at the interface region at different sputtering steps. The spectra are presented without additional post-processing beyond standard background subtraction. The low binding energy component is assigned to elemental Si (Si^0), while higher binding energy features correspond to oxidized Si–O species [18,21]. During depth profiling, the elemental Si component was used as an internal reference, as its binding energy remained stable within experimental uncertainty. In contrast, the SiO_2-related component exhibited binding energy shifts due to differential charging.

For depth profiling we have applied the default setting of the equipment which is: angle of incidence of 45°, area of sputtered region is 2 × 2 mm and standing sample. Monatomic Ar^+ ion with an energy of 0.5 keV and 6 keV Ar^+_{1000} and 8 keV $Ar^+_{1000/500/150}$ clusters were used for investigating the effect of different kinds of ion bombardments on the SiO_2/Si sample. Profiles using the same ion beam conditions were measured more than once and reasonable reproducibility was reached in all cases.

2.4. AFM measurements

The surface topography after removing the surface oxide layer was investigated by a Bruker Multimode 8 AFM equipped in tapping mode with a RTESPA-525 type tip mounted on a stainless-steel cantilever. Scan sizes of 3 × 3 μm were chosen for all samples, 3 different positions were measured. All AFM images were flattened using a second order polynomial in the X and Y directions to correct for curvature caused by piezo tube bowing.

3. Results

It is known that the conventional monatomic ion sputtering, typically Ar^+ ions can introduce significant artifacts such as interfacial broadening, preferential sputtering and atomic mixing. Cluster ion sputtering is known to preserve chemical bonds however its use for inorganic material is limited due to the low sputtering yield, therefore they are mainly used in depth profiling of organic and hybrid materials [22] Due to their lower energy per constituent atom and more distributed energy deposition, cluster ions can significantly reduce chemical modification and atomic mixing during sputtering. XPS enables clear distinction between fully oxidized Si^{4+} and reduced Si suboxide states (Si^+–Si^{3+}), making this system particularly well suited for assessing sputter-induced reduction, interface broadening, and depth resolution. The argon sputtering parameters with the corresponding energy/particle and the practically important required time for reaching the interface are summarized in Table 1.

The ion/cluster beam densities have not been measured. The values in Table 1 are the experimentally measured times required to reach the SiO_2/Si interface for various ion beam parameters applied in this work. Since the beam current density was not measured, these values cannot be converted into absolute sputter yields. Thus, the parameters shown in Table 1 should be only used for designing an experiment.

3.1. AFM data

Fig. 3 shows the AFM images obtained for the samples after removing ~15 nm layer thickness. The calculated RMS values together with

Table 1
Various argon sputtering parameters with the corresponding energy/particle.

Projectile	Energy (keV)	Energy/ particle (eV)	Time to reach the interface (s)
Ar^+	0.5	500	300
Ar^+_{1000}	6	6	3600
Ar^+_{1000}	8	8	1400
Ar^+_{500}	8	16	1260
Ar^+_{150}	8	53.3	1400

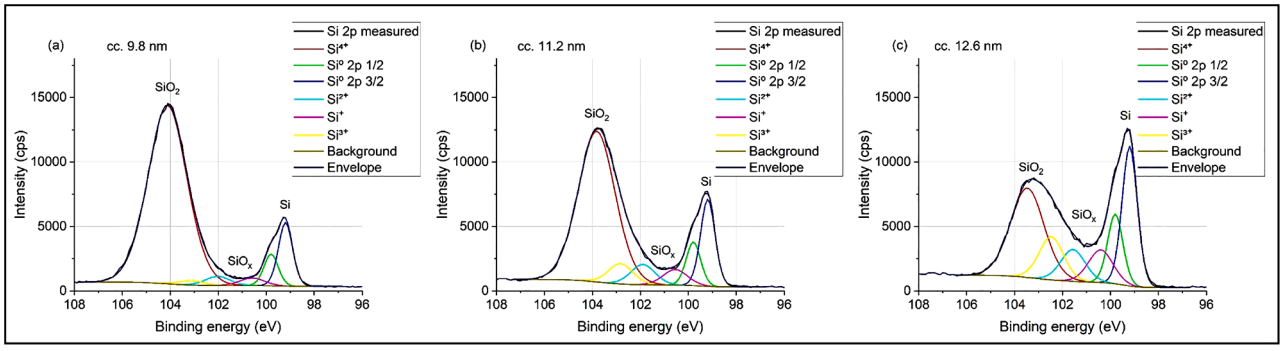

Fig. 2. Variation of the Si 2p peak in the interface region at various depths a. ~ 9.8 nm; b. ~ 11.2 nm; c. ~ 12.6 nm. Si^0 stands for elemental Si, Si^{4+} for Si in SiO_2, $Si^{+,\ 2+,\ 3+}$ for Si in SiO_x. For the details of decomposition see text.

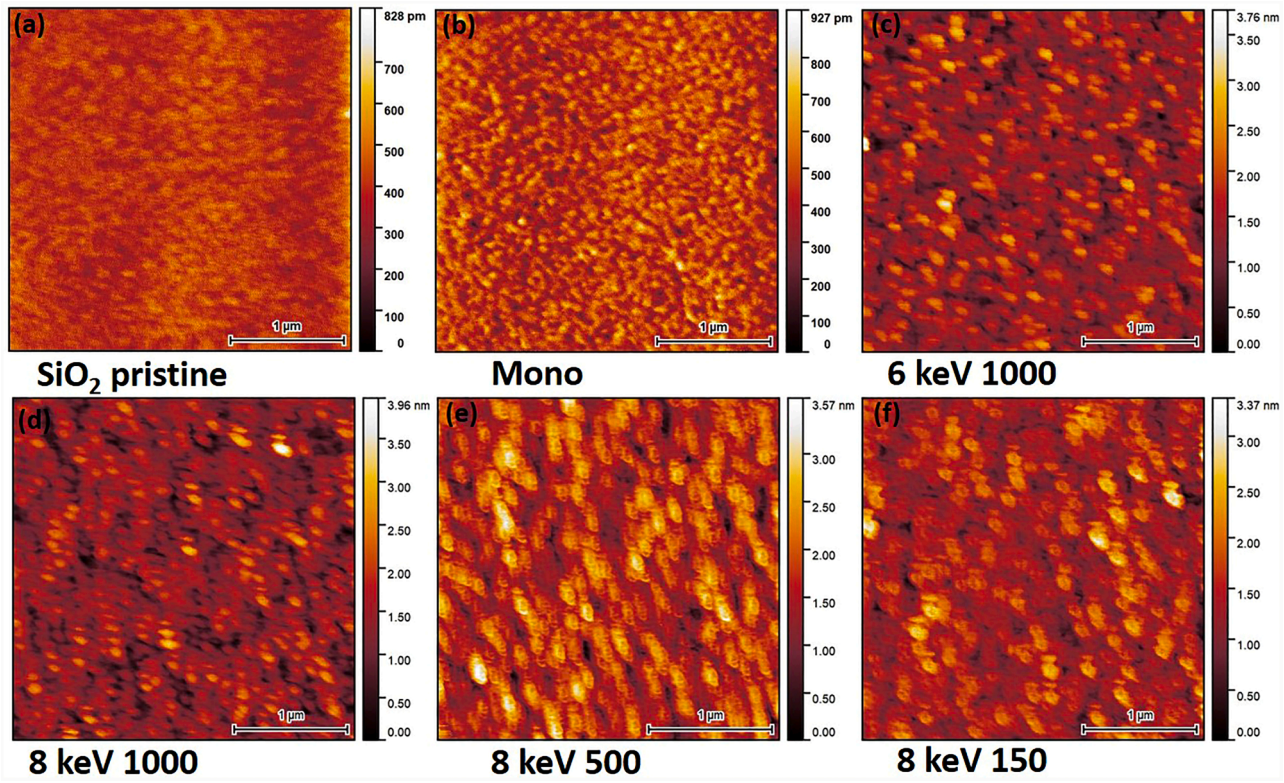

Fig. 3. Tapping mode AFM images a. SiO_2 pristine b. monatomic Ar^+ c. 6 keV Ar^+_{1000} d 8 keV Ar^+_{1000} e. 8 keV Ar^+_{500} f. 8 keV Ar^+_{150} sputtered samples.

statistical evaluation are provided in Table 2. The RMS roughness for the pristine samples is within sub-nanometer roughness regime reported for high-quality thermally grown SiO_2 films [23,24]. We can see that all ion bombardment applied increased the roughness of the sample. Monatomic sputtering increased the roughness slightly while cluster sputtering resulted in a much rougher surface. There are very limited studies on morphology development due to cluster sputtering. Shard et al. [25] investigated sputter induced morphologies on GaAs by SEM employing a rastered ion beam at an angle of 60° to the surface normal. They have shown that ripples do not form during 3 keV monoatomic argon sputtering in gallium arsenide, while during 8 keV Ar^+_{1000} argon cluster sputtering ripples were formed. Kyoung et al. [26] investigated Si/Ge multilayers on Si (100) single crystal by 20 keV Ar^+_{2500} cluster sputtering. They have shown the wave length of the ripples on the Si substrate being cc. 200 nm, which was perpendicular to the argon beam direction. Romanyuk et al. [27] have shown considerably roughness increase of GaP/Si(0 0 1) layers by 2.5 keV Ar^+_{2500} ions. Conard et al. [28] observed severe roughness increase in Al-delta layers embedded in a Si-matrix in the case of 10 keV Ar^+_{2673} sputtering. It is known that in the case of cluster sputtering high temperature and pressure transients are generated in the vicinity of impact [25,29]. In the case of cluster sputtering of the Si/SiO_2 system, these effects may contribute to the roughness increase.

Table 2
RMS values are reported as mean ± 95% confidence interval calculated from three AFM measurements acquired at different locations on each sample.

	Si pristine	Mono	6 keV 1000	8 keV 1000	8 keV 500	8 keV 150
RMS (nm)	0.070 ± 0.037	0.1 ± 0.019	0.4 ± 0.028	0.4 ± 0.058	0.5 ± 0.032	0.4 ± 0.076

3.2. XPS depth profiles

It is well known that the evaluation of the concentrations from the measured depth profiles in case of inhomogeneous concentration distribution is model dependent [26]. Thus, it is advisable to ignore system provided concentration calculation and instead to show the depth profiles based on the peak areas. The Si 2p and O 1 s lines were measured for depth profiling. The Si2p line was decomposed to Si^0, Si^+, Si^{2+}, Si^{3+} components. Depth profiles were made from the Si, pure Si, component and non-stoichiometric oxide components. In this work, "non--stoichiometric silicon oxide" refers to Si suboxide (this term will be used later) contribution identified in the Si 2p spectra, defined as the sum of the intermediate Si oxidation states Si^{1+}, Si^{2+} and Si^{3+}. These components represent SiO_x species with compositions between elemental Si and stoichiometric SiO_2. For comparison of the various depth profiles, one should normalize them. Luckily all depth profiles have reached the pure Si and thus this region could be used for normalization of the measured depth profile. The Si^o values measured in this region were normalized to that measured by monatomic bombardment and were called 100%. The normalization of horizontal axis (time or removed layer thickness) is a bit more difficult. First, we deal with the conversion of the sputter time to removed layer thickness. Degreve et al. [30] have shown that in case of low energy Ar^+ ion bombardment the sputter rate difference between SiO_2 and Si is only 4%, which can be neglected. Fig. 4a shows that the as measured profiles of the Si^0 using monatomic Ar^+ and 8/150 Ar cluster bombardments are rather similar, thus we think that in this case the difference of sputter rates is also low. Based on this observation even in the case of cluster bombardment we will neglect the sputter rate differences between the Si and SiO_2. Since the thickness of SiO_2 is known from the ellipsometry measurement, the conversion of sputter time to removed layer thickness is straightforward. Since the broadening either because of the ion mixing or the roughening is rather similar thus, we assume that at the interface the peak area reaches 50% [31]. The normalized experimentally determined depth profiles curves are shown in Fig. 4.

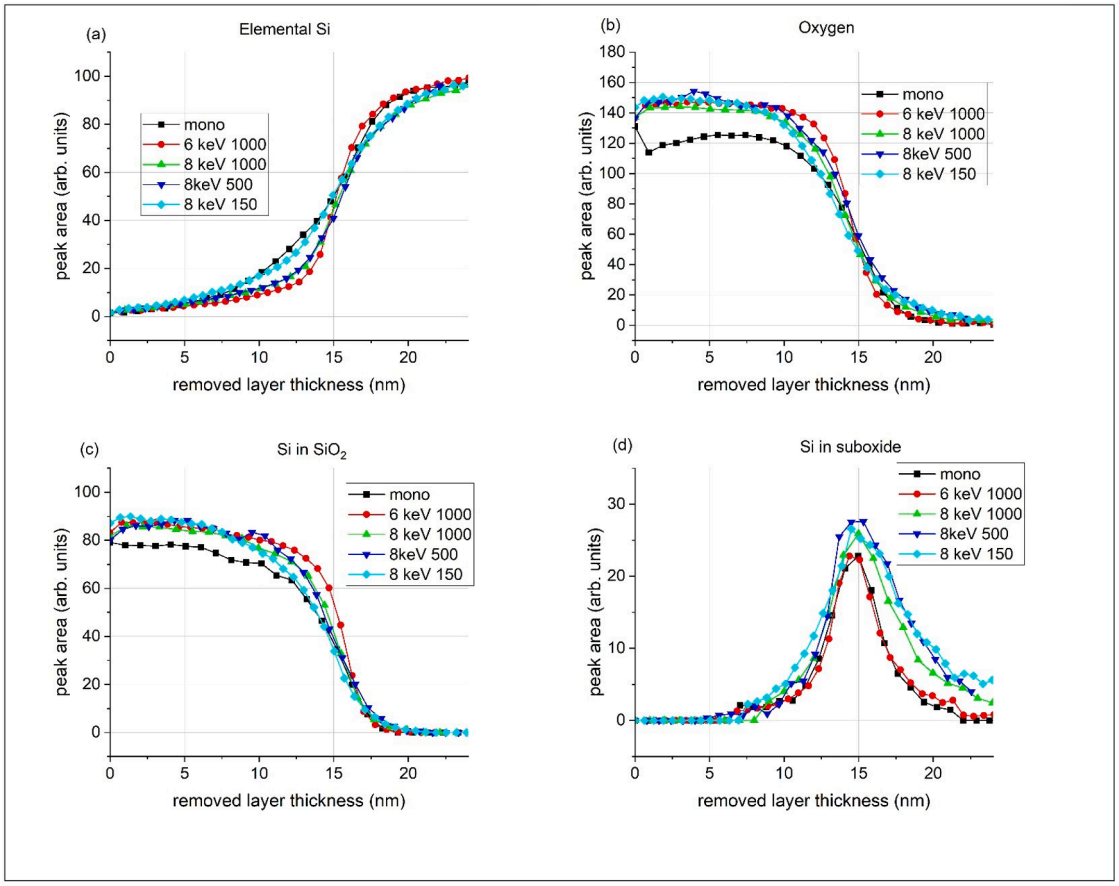

Fig. 4. The as measured depth profiles of a. elemental Si b. Oxygen, c. Si in SiO_2 and d. Si in suboxide The mono 6/1000, 8/1000, 8/500 and 8/150 stand for the projectiles produced the depth profiles. The Si in suboxide curves were shifted to have their maximum around 15 nm.

4. Discussions

The as measured XPS profiles (Fig. 4) show that the concentration distributions are inhomogeneous within the information depth of the XP electrons (5–12 nm), thus detailed evaluation of the depth profiles is necessary. Various approaches to cope with the problem are available [22]. In the following, different solutions, selected based on the type of ion bombardment induced alterations will be proposed.

4.1. *Si in suboxide (see Fig. 4d)*

According to Fig. 4d Si suboxide appeared in all depth profiles. It is known [32] that the Si/SiO_2 transition region might contain intermediate oxidation states (Si^{1+}–Si^{3+}), reflecting the gradual bonding transition between elemental Si and stoichiometric SiO_2. In addition, no carbon signal was detected at the interface, indicating that the observed Si suboxide species are not arising from carbon-containing interfacial contamination. In our case the amount and distribution of Si suboxide strongly depends on the applied bombardment, thus it cannot be an intrinsic feature of the interface. Thus, we conclude that the appearance of the Si suboxide is an artefact of the ion bombardment. Its production can be described in case of the monatomic bombardment (see 4.2) which shows that the Si suboxide formation occurs 1–3 nm distance under the instantaneous surface. In this situation the large inelastic mean free path (IMFP) of the photoelectron does not play any role; only a slight broadening occurs. Thus, the as measured profiles can be discussed without additional corrections. The lowest and similar Si suboxides are introduced by the monatomic and 6/1000 cluster bombardments, while in case of the other cluster bombardments a significantly greater amount of artefact production occurs. In case of monatomic bombardment there is plenty of energy to break chemical bonds, thus artefact production is not surprising [33,34].On the other hand, in case of cluster bombardment we do not expect bond breakage; this method was specifically introduced to avoid this problem. It seems, however, that in the interface region strong Si suboxide production occurs during cluster bombardment as well, and the damage increases with increasing energy/particle. Though we cannot give a complete explanation of the process we mention that molecular dynamics simulations have suggested that GCIB sputtering cannot always be described as a simple sequence of independent binary collisions. Instead, the collective impact of the cluster may generate localized high-pressure and high-temperature regions, leading to enhanced surface modification, suboxide formation and roughness development [35–37]. A more complex description of the process might be found if one also considers the individual suboxide (Si^{+}, Si^{2+}, Si^{3+}) depth profiles which are given in Supporting Information Fig. S1.

4.2. *Evaluation of Si^0 profile in case of monatomic bombardment (see Fig. 4a)*

The AFM image, Fig. 3b, shows that in case of monatomic 0.5 keV/45° ion bombardment the roughening is extremely low, it is in the range of 0.1 nm. Thus, the bombardment induced alteration is due to ion beam induced mixing. We will use the same procedure which is described in Ref [34]. Its essence is the following; first the ion mixing caused by the bombarding ion is calculated based on the TRIDYN simulation [30], then having the concentration distributions the XP signal is calculated based on the IMFP values neglecting the elastic scattering. The IMFP values applied in the present case are summarized in Table 3 [38,39].

The TRIDYN simulation was applied in several cases with good

Table 3
The applied IMFP values in nm.

Matrix	Si 2p	O 1s
Si	3.10	2.3
SiO_2	3.75	2.8

success [34,40,41]. In this case the simulation was applied with the default parameters except the relocation threshold energy of Si and surface binding energy of O, which were chosen to be 3.7 eV and 0.5 eV, respectively. Fig. 5 shows the comparison of the measured and simulated curves.

The reasonably good agreement between the measured and simulated curves approves the validity of our assumption that the broadening shown in the XPS depth profiles is explained by the ion bombardment induced ion mixing. It should be also noted that interface broadening visible on the XPS depth profile is considerable larger than the actual alteration due to the ion beam mixing, which is enhanced due to the high information depth of the photoelectrons. To demonstrate this Fig. 6 shows the TRIDYN simulated elemental Si distributions, which is the actual damage introduced by the ion bombardment, in the SiO_2 (14.7 nm) / Si substrate sample after various times of ion bombardment (0.5 keV Ar^+ / 45°).

Fig. 6 clearly shows that the size of the ion mixing effected zone is much lower than the broadening shown in the XP depth profile; really the interface structure, does not even affected by the ion bombardment, while the removed layer thickness is <9 nm.

4.3. Evaluation of the cluster depth profiles (see corresponding curves in Fig. 4a, b and c)

According to the AFM results, the roughening is considerably larger in the case of cluster bombardments than in case of monatomic bombardment. Based on this observation it might be assumed that in case of cluster bombardment the observed interface broadening is due to the surface roughening, which might be estimated by Gaussian broadening [42]. On the other hand, we have shown already (4.1) that the cluster bombardment also causes bond breaking, which is not easily involved in the simple topographical roughening. Thus, not knowing the actual mechanisms we cannot make an evaluation like that in 4.2., rather, simple naked eye observations must be accepted. The shape, "broadening", of the depth profile mainly depends on the IMFP of the photoelectrons and damage introduced by the applied ion bombardment. Since the IMFP is constant and only the introduced damage varies with the type of bombardment, the comparison of the shapes of the depth profiles give qualitative information on the damage introduced by the various bombardments.

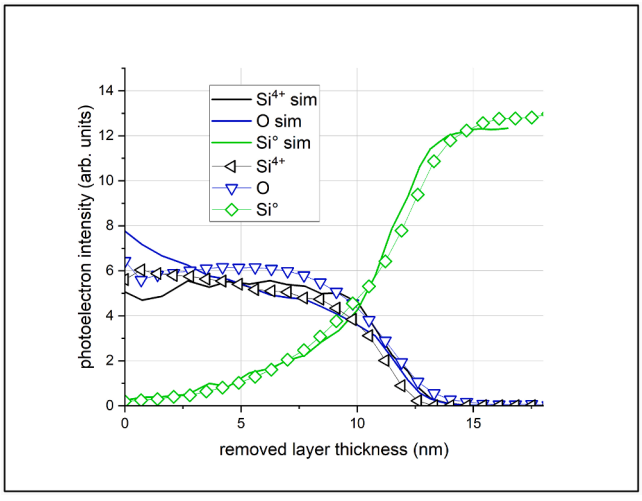

Fig. 5. The measured (markers) and simulated (lines) XP depth profiles of SiO_2 (14.7 nm) / Si substrate. Ion bombardment conditions: 0.5 keV monatomic Ar ion, angle of incidence 45° with respect to the surface normal.

Considering the Si^0 depth profiles belonging to various cluster bombardments (Fig. 4a) we can easily conclude that damage introduced by cluster bombardment scales with the energy/particle. The depth profiles belonging to the 8keV/150 cluster bombardment and monatomic bombardment are very much similar. This means that the overall damage of the two processes is similar. Presently we cannot explain this behavior because our understanding is that the mechanism of the two processes is strongly different.

The oxygen profiles (Fig. 4b) up to 10 nm removed layer thickness are similar, according to the expectation that the cluster bombardment will preserve chemical bonds, and cause only modest preferential sputtering etc. On the other hand, at the interface region the curves are separated and similarly to the previous scales with the particle/energy parameter. The reduction of oxygen (preferential sputtering) is the highest in the case of monatomic bombardment.

The Si in SiO_2 profiles (Fig. 4c) belonging to cluster bombardment scales with the energy/particles; the lowest damage was introduced by the 6keV/1000 cluster. The preferential sputtering in the case of monatomic bombardment is the strongest, accordingly the transformation of Si^{4+} to Si^0 is the highest, resulting in the lowest Si in SiO_2 signal.

Summarizing:

a. Artifact (Si suboxide) production (we have reported on similar problems [34]). This problem seems to be the most unwanted from the point of view of depth profiling. In this respect the best solution is the use of monatomic Ar ion and 6 keV Ar^+_{1000} bombardments, all others are less favorable.
b. Production of elemental Si. In this case the most problematic bombardments are the monatomic Ar ion and 8 keV Ar^+_{150} bombardments and the best is the 6 keV Ar_{1000} bombardment.
c. O distributions; reduction. All bombardments are similar, but the highest O reduction is caused by the monatomic Ar ion bombardment.

In addition to the above, one should also consider that the length of these depth profiling experiments is vastly different (300 s for monoatomic argon and between 1200–3600 s for cluster bombardment), which can be also an important parameter from practical point of view.

Based on the above, if one is interested in determining the possible presence of some suboxide layer on the interface, monatomic sputtering is to be used because it is much faster than that of 6 keV Ar^+_{1000}. If we are interested in the possible degradation in the SiO_2 layer, then the 8 keV Ar^+_{1000} cluster bombardment is to be used because though it is slightly more prone to defect production than that of 6 keV Ar^+_{1000} but its sputtering rate is far higher. Thus, we conclude that the formally best 6 keV Ar^+_{1000} cluster ion bombardment can be replaced without sacrificing information content.

All these conclusions, however, are based on the specific sample we discuss. One might ask what the situation would be if we used the gentle bombarding conditions described in this work, but the thickness of the SiO_2 layer is thicker or narrower than the present one. According to the presented study, the alteration can be described considering the processes of ion beam mixing and surface roughening. Ion beam mixing does not change with the thickness of the SiO_2 layer, thus it will not cause additional issues. On the other hand, if we consider the surface roughening the situation is much more confusing, even if we only deal with monatomic ion bombardment. The seminal paper of Bradley and Harper (BH) [43], which has been verified countless times, proposes an increasing roughness with increasing removed layer thickness. On the other hand having a perfect quality Si single crystal the surface roughness terminates at a low value [44]. In the case of cluster bombardment,

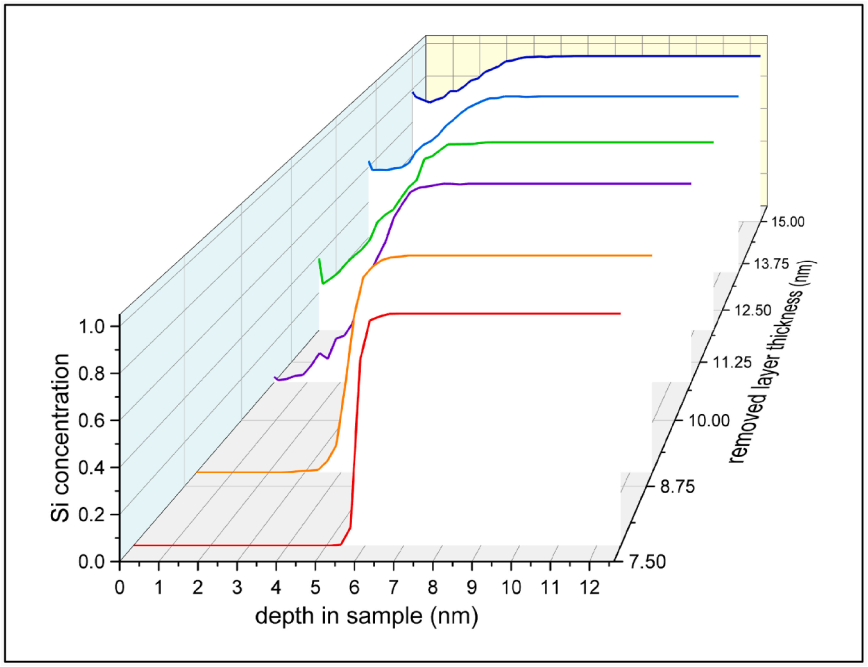

Fig. 6. The TRIDYN simulated Si distributions produced during depth profiling of SiO_2 (14.7 nm) / Si substrate sample (0.5 keV monatomic Ar^+ion, angle of incidence 45°) after removing various thicknesses.

we do not have such a rich data set on roughening vs removed layer thickness behavior. If we suppose that the roughening of the SiO_2 surface during cluster bombardment follows the BH theory, then cluster bombardment cannot be used for a thicker layer, but in case of a narrower layer it might be a good solution. Thus, while the evolution of roughness with bombardment time requires further investigation, the present results provide a consistent basis for comparing sputtering-induced modifications.

5. Conclusion

We have compared the XPS depth profiles of SiO_2/Si sample produced by various projectiles, namely monatomic 0.5 keV Ar^+ ion, and clusters of 6 keV Ar_{1000}, 8 keV $Ar_{1000,\ 500,\ 150}$. It was shown that in all cases the large broadening of the as measured transition is due to the large IMFP of the photoelectrons. In case of monatomic bombardment, the observed damage can be explained by ion mixing which can be described by TRIDYN simulation. In case of cluster bombardment the roughening might explain the alteration in the pure matrix, but also some new mechanism is active in the interface region. In details all applied ion bombardments produced Si suboxide (non-stoichiometric silicon oxide) formation in the interface region. The most dominant and lowest artefact production were found in the case of 8 keV Ar^+_{150} cluster; 6 keV Ar^+_{1000} cluster and monatomic 0.5 keV Ar ion bombardment, respectively. All applied ion bombardments caused reduction in the SiO_2 layer; the highest reduction was produced by the monatomic 0.5 keV Ar ion bombardment. Because of the large variety of damages, the choice of the best possible ion bombardment conditions must depend on the desired information.

CRediT authorship contribution statement

A.S. Racz: Writing – review & editing, Writing – original draft, Visualization, Validation, Methodology, Investigation, Formal analysis, Data curation, Conceptualization. **D. Olasz:** Investigation. **M. Menyhard:** Writing – review & editing, Writing – original draft, Visualization, Validation, Supervision, Methodology, Formal analysis, Data curation. **O. Krafcsik:** Writing – review & editing, Validation, Methodology, Formal analysis, Conceptualization.

Declaration of competing interest

The authors declare that they have no known competing financial interests or personal relationships that could have appeared to influence the work reported in this paper.

Acknowledgement

Thanks are given to R. Hodovan for producing the SiO_2 layers and to Z. Kovacs for FIB lamella production. Thanks are given for Dr. G. Dobrik for discussion and for providing AFM facility.

Supplementary materials

Supplementary material associated with this article can be found, in the online version, at doi:10.1016/j.apsadv.2026.101033.

Data availability

Data will be made available on request.

References

[1] M.P. Seah, S.J. Spencer, F. Bensebaa, I. Vickridge, H. Danzebrink, M. Krumrey, T. Gross, W. Oesterle, E. Wendler, B. Rheinländer, Y. Azuma, I. Kojima, N. Suzuki, M. Suzuki, S. Tanuma, D.W. Moon, H.J. Lee, H.M. Cho, H.Y. Chen, A.T.S. Wee, T. Osipowicz, J.S. Pan, W.A. Jordaan, R. Hauert, U. Klotz, C. Van Der Marel, M. Verheijen, Y. Tamminga, C. Jeynes, P. Bailey, S. Biswas, U. Falke, N.V. Nguyen, D. Chandler-Horowitz, J.R. Ehrstein, D. Muller, J.A. Dura, Critical review of the current status of thickness measurements for ultrathin SiO_2 on Si part V: results of a CCQM pilot study, Surf. Interface Anal. 36 (2004) 1269–1303, https://doi.org/10.1002/sia.1909.

[2] S.W. Glunz, F. Feldmann, SiO2 surface passivation layers – a key technology for silicon solar cells, Sol. Energy Mater. Sol. Cells 185 (2018) 260–269, https://doi.org/10.1016/j.solmat.2018.04.029.

[3] R.N. Kim, H.W. Yun, J. Lee, W.B. Kim, Dipole formation and electrical properties according to SiO_2 layer thickness at an Al_2O_3 /SiO_2 interface, J. Phys. Chem. C 125 (2021) 14486–14492, https://doi.org/10.1021/acs.jpcc.1c03730.

[4] C. Zhang, T. Qi, W. Wang, C. Zhao, S. Xu, M. Ma, Y. Feng, W. Li, M. Chen, C. Yang, W. Li, High efficiency CIGS solar cells on flexible stainless steel substrate with SiO2

diffusion barrier layer, Sol. Energy 230 (2021) 1033–1039, https://doi.org/10.1016/j.solener.2021.11.006.
[5] D.R. Baer, M.H. Engelhard, A.S. Lea, P. Nachimuthu, T.C. Droubay, J. Kim, B. Lee, C. Mathews, R.L. Opila, L.V. Saraf, W.F. Stickle, R.M. Wallace, B.S. Wright, Comparison of the sputter rates of oxide films relative to the sputter rate of SiO2, J. Vac. Sci. Technol. Vac. Surf. Films 28 (2010) 1060–1072, https://doi.org/10.1116/1.3456123.
[6] J. Matsuo, M. Akizuki, J. Northby, G.H. Takaoka, I. Yamada, Sputtering with gas cluster-ion beams, Surf. Rev. Lett. 03 (1996) 1017–1021, https://doi.org/10.1142/S0218625X96001820.
[7] I. Yamada, Materials processing by gas cluster ion beams, Mater. Sci. Eng. R Rep. 34 (2001) 231–295, https://doi.org/10.1016/S0927-796X(01)00034-1.
[8] Z. Lin, X. Li, G. Chen, P. Zhang, Y. Cao, L. Ren, H. Shao, X. Zhao, A review of material surface processing utilizing gas cluster ion beam technology, Eur. Phys. J. D 79 (2025) 50, https://doi.org/10.1140/epjd/s10053-025-01002-0.
[9] T. Miyayama, N. Sanada, M. Suzuki, J.S. Hammond, S.Q.D. Si, A. Takahara, X-ray photoelectron spectroscopy study of polyimide thin films with Ar cluster ion depth profiling, J. Vac. Sci. Technol. Vac. Surf. Films 28 (2010) L1–L4, https://doi.org/10.1116/1.3336242.
[10] Y.Y. Chen, B.Y. Yu, W.B. Wang, M.F. Hsu, W.C. Lin, Y.C. Lin, J.H. Jou, J.J. Shyue, X-ray photoelectron spectrometry depth profiling of organic thin films using C_{60} sputtering, Anal. Chem. 80 (2008) 501–505, https://doi.org/10.1021/ac701899a.
[11] R. Simpson, R.G. White, J.F. Watts, M.A. Baker, XPS investigation of monatomic and cluster argon ion sputtering of tantalum pentoxide, Appl. Surf. Sci. 405 (2017) 79–87, https://doi.org/10.1016/j.apsusc.2017.02.006.
[12] M.C. Burrell, E. Gillman, XPS investigation of monoatomic and cluster argon sputtering of zirconium dioxide, J. Vac. Sci. Technol. A 41 (2023) 043202, https://doi.org/10.1116/6.0002630.
[13] A.J. Barlow, J.F. Portoles, P.J. Cumpson, Observed damage during Argon gas cluster depth profiles of compound semiconductors, J. Appl. Phys. 116 (2014) 054908, https://doi.org/10.1063/1.4892097.
[14] R. Steinberger, J. Sicking, J. Weise, J. Duchoslav, T. Greunz, D.C. Meyer, D. Stifter, Chemical degradation of selected Zn-based corrosion products induced by C60 cluster, Ar cluster and Ar+ ion sputtering in the focus of X-ray photoelectron spectroscopy (XPS), Appl. Surf. Sci. 403 (2017) 15–22, https://doi.org/10.1016/j.apsusc.2017.01.105.
[15] D. Aureau, K. Ridier, B. Bérini, Y. Dumont, N. Keller, J. Vigneron, M. Bouttemy, A. Etcheberry, A. Fouchet, Advanced analysis tool for X-ray photoelectron spectroscopy profiling: cleaning of perovskite SrTiO3 oxide surface using argon cluster ion source, Thin Solid Films 601 (2016) 89–92, https://doi.org/10.1016/j.tsf.2015.11.017.
[16] Y.K. Kyoung, J.G. Chung, H.I. Lee, D. Yun, J.C. Lee, Y.S. Kim, S.K. Oh, H.J. Kang, Electronic structures of SiO_2 thin films via Ar gas cluster ion beam sputtering, Surf. Interface Anal. 46 (2014) 58–61, https://doi.org/10.1002/sia.5460.
[17] J.B. Malherbe, S. Hofmann, J.M. Sanz, Preferential sputtering of oxides: a comparison of model predictions with experimental data, Appl. Surf. Sci. 27 (1986) 355–365, https://doi.org/10.1016/0169-4332(86)90139-X.
[18] F.J. Himpsel, F.R. McFeely, A. Taleb-Ibrahimi, J.A. Yarmoff, G. Hollinger, Microscopic structure of the SiO 2 /Si interface, Phys. Rev. B 38 (1988) 6084–6096, https://doi.org/10.1103/PhysRevB.38.6084.
[19] J.W. Keister, J.E. Rowe, J.J. Kolodziej, H. Niimi, H.S. Tao, T.E. Madey, G. Lucovsky, Structure of ultrathin SiO2/Si(111) interfaces studied by photoelectron spectroscopy, J. Vac. Sci. Technol. Vac. Surf. Films 17 (1999) 1250–1257, https://doi.org/10.1116/1.581805.
[20] Copyright © 2005 Casa Software Ltd, (n.d.). http://www.casaxps.com/(accessed July 18, 2023).
[21] L. Zhang, N. Kuramoto, Y. Azuma, A. Kurokawa, K. Fujii, Thickness measurement of oxide and carbonaceous layers on a^{28} Si sphere by XPS, IEEE Trans. Instrum. Meas. 66 (2017) 1297–1303, https://doi.org/10.1109/TIM.2016.2634678.
[22] A.S. Racz, M. Menyhard, Evaluation methods for XPS depth profiling; A review, Appl. Surf. Sci. Adv. 30 (2025) 100872, https://doi.org/10.1016/j.apsadv.2025.100872.
[23] X. Blasco, D. Hill, M. Porti, M. Nafría, X. Aymerich, Topographic characterization of AFM-grown SiO_2 on Si, Nanotechnology 12 (2001) 110–112, https://doi.org/10.1088/0957-4484/12/2/307.
[24] K. Ohsawa, Y. Hayashi, R. Hasunuma, K. Yamabe, Roughness increase on surface and interface of SiO_2 grown on atomically flat Si (111) terrace, J. Phys. Conf. Ser. 191 (2009) 012031, https://doi.org/10.1088/1742-6596/191/1/012031.
[25] A.G. Shard, M.A. Baker, Practical guides for x-ray photoelectron spectroscopy: use of argon ion beams for sputter depth profiling and cleaning, J. Vac. Sci. Technol. A 42 (2024) 050801, https://doi.org/10.1116/6.0003681.
[26] Y.K. Kyoung, H.I. Lee, J.G. Chung, S. Heo, J.C. Lee, Y.J. Cho, H.J. Kang, Damage profiles of Si (001) surface via Ar cluster beam sputtering, Surf. Interface Anal. 45 (2013) 150–153, https://doi.org/10.1002/sia.4917.
[27] O. Romanyuk, I. Gordeev, A. Paszuk, O. Supplie, J.P. Stoeckmann, J. Houdkova, E. Ukraintsev, I. Bartoš, P. Jiříček, T. Hannappel, GaP/Si(0 0 1) interface study by XPS in combination with Ar gas cluster ion beam sputtering, Appl. Surf. Sci. 514 (2020) 145903, https://doi.org/10.1016/j.apsusc.2020.145903.
[28] T. Conard, C. Fleischmann, R. Havelund, A. Franquet, C. Poleunis, A. Delcorte, W. Vandervorst, Inorganic material profiling using Arn+ cluster: can we achieve high quality profiles? Appl. Surf. Sci. 444 (2018) 633–641, https://doi.org/10.1016/j.apsusc.2018.02.159.
[29] F. Musumeci, H. Ryuto, A. Sakata, M. Takeuchi, G.H. Takaoka, Spectroscopic evidences of high temperatures and pressures during the cluster ion beam interaction with solid surfaces, J. Lumin. 172 (2016) 224–230, https://doi.org/10.1016/j.jlumin.2015.12.018.
[30] F. Degreve, Ph. Ged, SIMS study of the SiO_2 /Si interface and of the Si+O_2 system, Surf. Interface Anal. 5 (1983) 83–86, https://doi.org/10.1002/sia.740050206.
[31] H.J. Mathieu, Thin film depth profile Anal, in: H. Oechsner (Ed.), Depth Profile and Interface Analysis of Thin Films by AES and XPS, Springer Berlin Heidelberg, Berlin, Heidelberg, 1984, pp. 39–61, https://doi.org/10.1007/978-3-642-46499-7_3.
[32] G. Hollinger, F.J. Himpsel, Probing the transition layer at the SiO2-Si interface using core level photoemission, Appl. Phys. Lett. 44 (1984) 93–95, https://doi.org/10.1063/1.94565.
[33] A.S. Racz, Z. Fogarassy, P. Panjan, M. Menyhard, Evaluation of AES depth profiles with serious artefacts in C/W multilayers, Appl. Surf. Sci. 582 (2022) 152385, https://doi.org/10.1016/j.apsusc.2021.152385.
[34] A.S. Racz, M. Menyhard, XPS depth profiling of nano-layers by a novel trial-and-error evaluation procedure, Sci. Rep. 14 (2024) 18497, https://doi.org/10.1038/s41598-024-69495-0.
[35] A. Delcorte, N. Wehbe, P. Bertrand, B.J. Garrison, Sputtering of organic molecules by clusters, with focus on fullerenes, Appl. Surf. Sci. 255 (2008) 1229–1234, https://doi.org/10.1016/j.apsusc.2008.05.107.
[36] Z. Postawa, L. Rzeznik, R. Paruch, M.F. Russo, N. Winograd, B.J. Garrison, Depth profiling by cluster projectiles as seen by computer simulations, Surf. Interface Anal. 43 (2011) 12–15, https://doi.org/10.1002/sia.3417.
[37] B.J. Garrison, Z. Postawa, Computational view of surface based organic mass spectrometry, Mass Spectrom. Rev. 27 (2008) 289–315, https://doi.org/10.1002/mas.20165.
[38] QUASES-IMFP-TPP2M - QUASES, (n.d.). http://www.quases.com/products/quases-imfp-tpp2m/(accessed June 7, 2023).
[39] S. Tanuma, C.J. Powell, D.R. Penn, Calculations of electron inelastic mean free paths. V. Data for 14 organic compounds over the 50-2000 eV range, Surf. Interface Anal. 21 (1994) 165–176, https://doi.org/10.1002/sia.740210302.
[40] A.S. Racz, Z. Fogarassy, U. Kentsch, P. Panjan, M. Menyhard, Design and production of tungsten-carbide rich coating layers, Appl. Surf. Sci. 586 (2022) 152818, https://doi.org/10.1016/j.apsusc.2022.152818.
[41] A.S. Racz, M. Menyhard, Design of corrosion resistive SiC nanolayers, ACS Appl. Mater. Interfaces 10 (2018) 22851–22856, https://doi.org/10.1021/acsami.8b06425.
[42] S. Hofmann, Sputter depth profiling: past, present, and future: sputter depth profiling: past, present, and future, Surf. Interface Anal. 46 (2014) 654–662, https://doi.org/10.1002/sia.5489.
[43] R.M. Bradley, J.M.E. Harper, Theory of ripple topography induced by ion bombardment, J. Vac. Sci. Technol. Vac. Surf. Films 6 (1988) 2390–2395, https://doi.org/10.1116/1.575561.
[44] S.A. Pahlovy, S.F. Mahmud, K. Yanagimoto, N. Aikawa, I. Miyamoto, Roughening and smoothing behavior of single crystal Si by low energy Ar+ ion bombardment, Nucl. Instrum. Methods Phys. Res. Sect. B Beam Interact. Mater. At. 272 (2012) 206–209, https://doi.org/10.1016/j.nimb.2011.01.066.